2020 IEEE/RSJ International Conference on Intelligent Robots and Systems (IROS)
October 25-29, 2020, Las Vegas, NV, USA (Virtual)

Emergent adaptive gait generation through Hebbian sensor-motor maps by morphological probing

Matthieu Dujany*, Simon Hauser*, Mehmet Mutlu*†, Martijn van der Sar*,
Jonathan Arreguit*, Takeshi Kano‡, Akio Ishiguro‡ and Auke Ijspeert*
*Biorobotics Laboratory (BioRob), EPFL, Lausanne, Switzerland, Email: matdujany@gmail.com
†Computer and Robot Vision Laboratory (Vislab), IST, Lisboa, Portugal
‡Research Institute of Electrical Communication, Tohoku University, Sendai, Miyagi, Japan

***Abstract*—Gait emergence and adaptation in animals is unmatched in robotic systems. Animals can create and recover locomotive functions "on-the-fly" after an injury whereas locomotion controllers for robots lack robustness to morphological changes. In this work, we extend previous research on emergent interlimb coordination of legged robots based on coupled phase oscillators with force feedback terms. We investigate how the coupling weights between these phase oscillators can be extracted from the morphology with a fast and computationally lightweight method based on a combination of *twitching* and Hebbian learning to form sensor-motor maps. The coefficients of these maps create naturally scaled weights, which not only lead to robust gait limit cycles, but can also adapt to morphological modifications such as sensor loss and limb injuries within a few gait cycles. We demonstrate the approach on a robotic quadruped and hexapod.**

***Index Terms*—locomotion, gait emergence, gait adaptation, modular robots, phase oscillators, twitching, Hebbian learning**

I. Introduction

Animals possess a remarkable ability to quickly recover their locomotion ability after unexpected morphological changes. An injured leg can lead to a temporary disabled normal locomotion control. Yet, it seems that the animal can "instantaneously" create a new locomotion strategy to accommodate the morphological modification, which could be motivated by survival needs (escaping from a predator). The method of finding a new controller seems to be through a highly efficient trial-and-error phase [1].

In robotics, such adaptation capabilities in the case of morphological modifications are challenging. Locomotion controllers for legged robots are usually designed on a model of the robot in a physics simulator. This normally involves a lengthy optimization procedure where up to hundreds or thousands of controllers are being tested. The output of the optimization process is a controller that is *tailored* to the specific morphology, and unless trained for such a case, is unlikely to have the capability to deal with modifications on the morphology. This means that every change in the morphology needs a reoptimization process, requiring significant computation and a flexible simulation environment.

Previous research dealing with gait adaptation due to morphological changes in real robotic hardware is rare. In [2], researchers built a model of a hexapod in simulation whose leg configurations could easily be modified. Then, they simulated millions of morphological modifications and let an optimization process find a viable controller for every one of them, creating an enormous database of potential controllers. The real hexapod robot was provided with this database, and after a morphological modification unknown to the controller could recover its locomotion capability in only a few trial-and-errors due to an efficient way of searching the database for the best match. Although applicable to any robot, this "brute force" approach leans on the reoptimization process described above, and it is unlikely that animals keep an explicit model of all morphological modifications.

The research in [3] also employs a model and simulations, but in a more on-the-fly scenario and with incorporating sensory feedback. After a morphological modification of a real

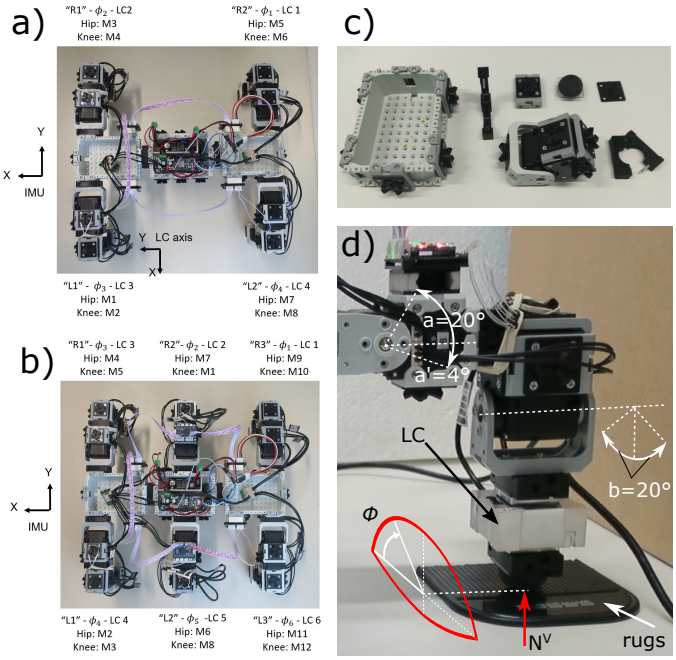

Fig. 1. a) Quadruped, b) Hexapod, c) modular parts, d) limb with phase oscillator parameters.

quadruped robot, it creates a small number of internal models. It then performs an action in both the simulation and the real world to rule out incorrect models and fine tune promising ones until a final internal model matches the modified structure in terms of sensor responses based on the performed actions. The method again only requires a few trials, however it is unclear if it can be applied to more complex morphologies due to the computationally expensive creation and simulation of the internal model. Animals in an emergency situation cannot afford to spend such excessive computational effort into finding a new locomotion strategy ad hoc. Moreover, the famous studies on decerebrated cats [4] showed that the brain is not needed in gait adaptation which thus seems inherently decentralized; the spinal cord can deal with such tasks in a quick and efficient manner.

An interesting research in this direction is presented in [5] where sensory feedback acts on phase oscillators that drive each leg of a hexapod. The load in stance of each leg can modulate the phase progression of its own and its neighboring legs. This feedback allows the structure to instantaneously react to a morphological change because of a different loading scenario, which the robot uses to find a new gait for the adapted morphology in an emergent manner.

Likewise, in [6], a decentralized control mechanism relying only on sensory feedback enables a star-like robot to adapt to multiple limbs amputations. For each limb, the sensory feedback produced in response to random movements enables to determine whether that limb should perform a power stroke to move the whole body and in which direction.

In this paper, we extend the research in [5] by developing a general method to learn from the morphology the appropriate coupling weights between sensory feedback and the limb phase oscillators to form an adaptive locomotion controller. Spontaneous Motor Activity (SMA, or *twitching*) is used to probe the morphology, during which Hebbian learning is used to form a connection between motor actions and sensory feedback. After this initial learning phase, our robot is able to demonstrate gait emergence and adaptation to a variety of morphological changes and sensor failures during runtime within a few locomotion cycles. Our method is fast and computationally light: the learning is performed by a simple microcontroller which also runs the final locomotion controller. Our goal is to imitate the "spinal cord" with a scalable and computationally lightweight framework.

II. Concept overview

A. Gait emergence with "Tegotae"

Tegotae [5, 7, 8] is a method to obtain emergent interlimb synchronization in locomotion, using distributed oscillators modulated by local sensory feedback, typically ground reaction forces. In [7], it is shown that with the simple rule presented in eq. (1), a walking gait can emerge in a quadruped robot. Each limb phase ϕ_i is updated using only the local sensory feedback N_i^V (the ground reaction normal force, see Fig. 1d for details) and a constant descending drive ω:

$$\dot{\phi}_i = \omega - \sigma N_i^V \cos(\phi_i). \quad (1)$$

In [5], this rule is further refined for a hexapod robot, by adding the sensory feedback from the other limbs:

$$\dot{\phi}_i = \omega - \sigma_1 N_i^V \cos(\phi_i) + \sigma_2 (\frac{1}{n_L} \sum_{j \in L(i)}^{n_L} k_j N_j^V) \cos(\phi_i). \quad (2)$$

Each limb has a limb-specific neighborhood $L(i)$ of n_L limbs whose influence on its phase update are set by the constants k_j. Starting from the expression of the Tegotae rule from [5], we propose the following generalization for any morphology:

$$\dot{\phi}_i = \omega + \sigma (\sum_{all\ j} k_{i,j} N_j^V) \cos(\phi_i). \quad (3)$$

In [5], the coefficients $k_{i,j}$ - or matrix $\mathbf{K}$ - were hand tuned. However, the idea presented in this paper is that these coefficients are related to the morphology through the neighboring function and their magnitude, and thus intuitively could be provided directly by the morphology [9].

The proposed approach aims at automatically finding the generalized Tegotae coefficients through locally probing the morphology and learning a causal relationship to the received sensory response. This local probing of the morphology is inspired from motor twitching.

B. Spontaneous Motor Activity

Motor twitching (or *Spontaneous Motor Activity*) is the sudden activation of single muscles against a background of muscle atonia, generating abrupt impulsive movements. This happens at the prenatal stage in the embryo, but also during REM sleep of mammals [10]. At first sight random, it has been shown that the twitching movements of new born rats are structured in spatiotemporal patterns and have motor developmental functions [11]. This is thought to be achieved by relating the induced movement to the provoked proprioceptive sensory response.

Using simple Hebbian learning rules, the self-organization properties of twitching on the reflex networks have been demonstrated for the nociceptive withdrawal reflex of rats tails in [12] and for a simulated leg in [13] and [10].

Inspired from these results, the proposed approach uses Hebbian learning during motor twitching to learn the generalized Tegotae coefficients $k_{i,j}$ from eq. (3).

III. Materials and Methods

A. Robotic platform

1) Mechanics: The goal in the future is to demonstrate that the approach presented here is applicable to a variety of legged morphologies. Hence, a modular robotic platform was developed that allows for a rapid manual reconfiguration. The basis of the platform is formed by the commercially available Bioloid Kit from Robotis (www.robotis.com) with hinged 1 Degree of Freedom (DoF) servo motors (Dynamixel

AX-12A) and passive structural body parts. These parts can be screwed together to form desired morphologies. To further accelerate the building process and allow more flexibility in the attachments of the modular parts, we designed a special male-female-male connector. Two male connectors lock together in 90 degree increments, and a female cuff wraps around and secures the configuration with a single screw. Each servo motor is equipped with up to 5 and each structural passive part with up to 8 connectors. We also added a half-sphere made out of rubber (Tango Black Shore A50) equipped with the same connector which is used as a foot. A morphology generally consists of passive body parts with in-series connected servo motors serving as actuated limbs with a rubber foot as the end effector. Fig. 1c shows details of the modified kit.

2) Sensors: The method presented in this work relies on sensory feedback, namely force feedback in the foot contacts and information about the global movement of the structure. Keeping overall simplicity in mind, we chose 3 axis load cells (LCT LAN-X1) with a relatively small form factor as force sensors, and an IMU (Sparkfun Razor IMU M0) with a triple axis accelerometer and a triple axis gyroscope as a movement sensor. Only one IMU is used, located in the middle of the structure. Tanks to the special connector, the load cells number and location in the structure is flexible.

3) Electronics: A Robotis OpenCM9.04 board is used to control the servo motors and to collect and process the sensory information. The board communicates with up to 256 servo motors via broadcasting. To enable an equally flexible setup for collecting data from the load sensors and IMU, a serial communication framework has been developed where each sensor acts in a daisychain. The full control loop runs at 50 Hz. A bluetooth module (JY-MCU) is connected to the main board to allow controlling the robot with a bluetooth enabled smartphone. A robot is either powered by an external power supply or by an on-board Li-Po battery (Conrad energy BEC 11.1 V 1300 mAh 12 C).

4) Morphologies: For this study, the overall complexity of the morphologies was kept relatively simple. Limbs consist of two servo motors in series, one acting as a "hip" and one acting as a "knee". Each limb contains one load cell to which the rubber foot is attached. Each morphology must contain the main "body" part, containing the main board, IMU, bluetooth module and optional battery; we call this element the "spinal cord". Following this design, we assembled two morphologies: a quadruped and a hexapod (Fig. 1a and 1b).

5) Phase oscillators: The motors within each limb are controlled by phase oscillators. The relationships between the angles of the limb servomotors (α_{knee} and α_{hip}) and the limb phase ϕ are as follows :

$$\alpha_{knee} = \pm a \cdot cos(\phi) \tag{4}$$

$$\alpha_{hip} = \pm b \cdot sin(\phi). \tag{5}$$

The sign correction is added so that the hip motors go to swing between 0 and π and to stance between π and 2π and so that the knee motors push in the desired locomotion direction when the limb is in stance.

B. Learning method

1) Twitching and sensor logging: The twitching is performed around a "neutral" stance position where all the motor angles are set to 0. The servo motors stiffness is set so that the motors can hold the structure but do not block an induced movement (compliance margin of 15° of the AX-12A servo motors), thus reproducing the muscle atonia characteristic of the REM sleep and of the embryo. During twitching, it is crucial that the movement of a twitch only progresses through the body and is not dissipated through other ways, namely slipping of the feet, as this negates proper sensory responses. For this reason, the robot was put on rubber rugs with a high friction coefficient during the learning process. Successively, each motor twitches bidirectionally following a ramp of $\pm 10^\circ$ over 500 ms. During each twitch, the position feedback from all the servo motors and the data stream from all sensors are sent to a desktop PC and recorded with MATLAB. This PC connection is solely used for recording purposes, all computations (learning and locomotion) are performed on board by the microcontroller. With a sampling time of 20 ms, 25 samples are collected and filtered (causal moving average filter of size 5). After each motor movement, all motors are centered back to the learning position.

2) Hebbian learning during motor twitching: Similarly to [12], [13] and [10], our learning rule (6) uses differential Hebbian learning [14] with a self-regulating term to learn the effects of each motor on each sensor, inspired from Oja's rule [15], i.e.

$$\Delta w_{i,j} = \eta(\dot{m}_j * \dot{s}_i - \dot{m}_j{}^2 * w_{i,j}). \tag{6}$$

In (6), $\Delta w_{i,j}$ is the update of the learnt weights at each step, η is the learning rate, $\dot{m}_j$ is the differentiated input, and $\dot{s}_i$ is the differentiated output.

In our case, m_j are the motor positions, which are differentiated to obtain $\dot{m}_{j\_motor}$. The sensory outputs s_i are defined as the force in local x-, y- and z-direction in the load cells $s_{i\_load\_xyz}$, the global rotation angles roll (r), pitch (p) and yaw (y) $s_{i\_rot\_rpy}$ and the global coordinates x, y, and z of the body $s_{i\_pos\_xyz}$. Sensory feedback from the load cells thus are differentiated to obtain $\dot{s}_{i\_load\_xyz}$, however the acceleration measurement of the IMU (as the double derivative of global position) is *integrated* to obtain $\dot{s}_{i\_pos\_xyz}$ and the gyroscope directly provides $\dot{s}_{i\_rot\_rpy}$.

Fig. 2a gives an example of each type of the raw and processed signals collected from one bidirectional twitch.

The learning rate η was tuned to obtain convergence (see Fig. 2b) in 5 cycles, i.e. each motor twitches five times in both directions. It can be seen that convergence from the load cells and gyroscope is stable, however convergence of the speed weights is inconsistent because the integrated accelerometer provides a noisy measure of speed, even with filtering.

At the end of the Hebbian learning process, we obtain a $(3n_{LC} + 6)$x$(2n_{motors})$ matrix. The directions of movement were split during the learning. However, if linearization assumptions hold around that position, the values in the two

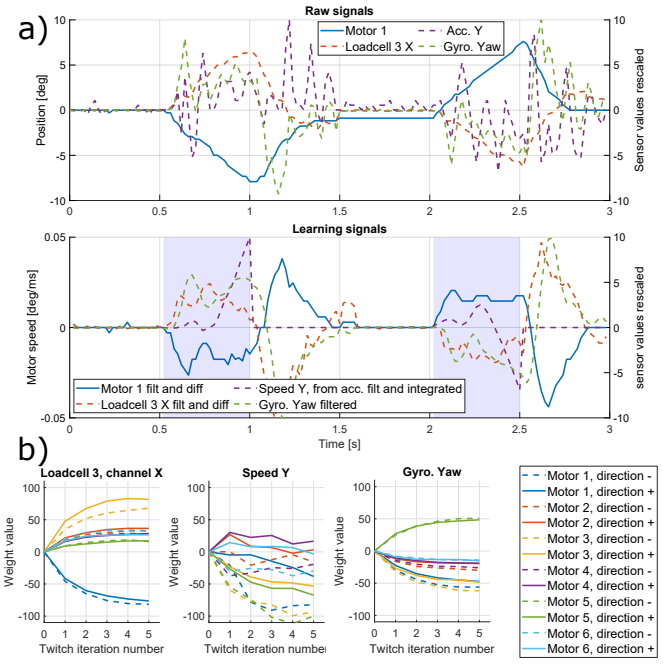

Fig. 2. a) Twitching signals obtained with quadruped structure. The twitching motor is motor 1 and the load cell is load cell 3 (load cell of the same limb). Learning happens only with the samples collected in the blue shaded area. b) Weights convergence for quadruped. Only load cell 3 channel X, speed in Y, gyroscope Yaw and motors M1 to M6 are plotted for clarity.

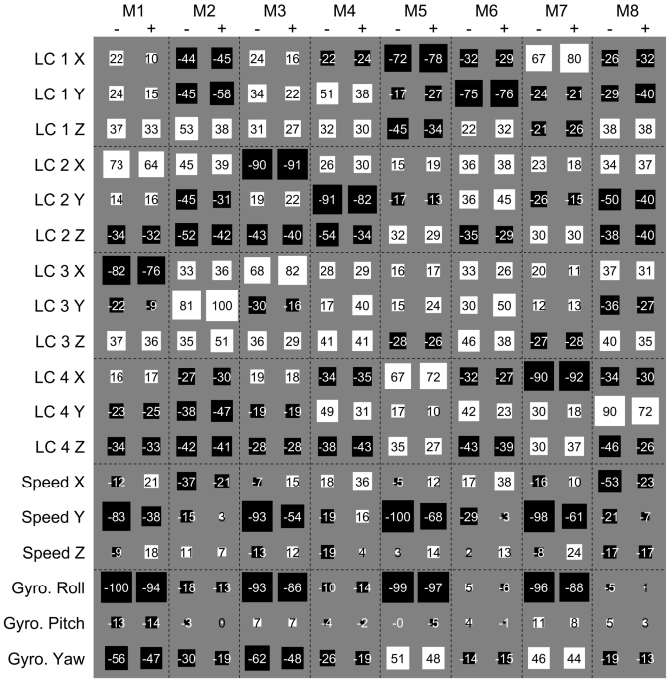

Fig. 3. Weights matrix learnt with quadruped structure. The weights have been rescaled from 0 to 100 in absolute value within their own group (load signals, gyro signals and speed signals).

directions should be the same. For the further processes, we formed the average of both directions. The resulting matrix shows the local response of differentiated sensory feedback to differentiated motor movement. Due to this in essence being $\partial s_i / \partial m_j$, we call this matrix the "Jacobian" around the learning position. Fig. 3 shows the original matrix for the quadruped structure (for space reasons the hexapod Jacobian is omitted). In both cases, the values are very similar in the two directions, except for the speed because of the noise in the accelerometer measurements.

Each twitch movement lasts 500ms, with 1s delays between the twitch movement for recentering and stabilization. With 8 motors (quadruped) and 10 twitches movement per motor (5 cycles of 2 directions), the learning is fully completed in just 2 minutes.

3) Information progression through the body: The method of learning from probing the morphology is based on the assumption that sensory feedback caused by a local perturbation declines over the spatial dimension of the body, i.e. a sensor spatially closer to the perturbation responds "higher" than the same sensor spatially further to the same perturbation. This is intuitive, as a local perturbation should not significantly affect parts further away. This is the key idea behind computing the neighboring function: the spatial declining of sensory response can automatically result in the neighboring function with correctly scaled Tegotae coefficients. As a validation for this assumption, we compute the absolute overall impact a motor twitch has on each of the load cells, i.e.

$$i_{LC}(m) = \sqrt{w_{LC_X,m}^2 + w_{LC_Y,m}^2 + w_{LC_Z,m}^2} \qquad (7)$$

and list the obtained values in Fig. 4a for the quadruped and in Fig. 4b for the hexapod. As an example, the first value 43 computes with $\sqrt{\frac{22+10}{2}^2 + \frac{24+15}{2}^2 + \frac{37+33}{2}^2}$. Green entries signify that the highest sensory response was correctly detected in the closest sensor to the twitch, i.e. the load cell in the limb where a motor twitched.

	M1	M2	M3	M4	M5	M6	M7	M8
LC 1	43	82	45	59	88	86	80	59
LC 2	78	73	102	101	38	63	42	70
LC 3	88	106	85	57	37	65	34	60
LC 4	44	66	39	67	78	60	100	94

(a) Quadruped

	M1	M2	M3	M4	M5	M6	M7	M8	M9	M10	M11	M12
LC 1	41	23	49	22	18	28	25	52	91	102	38	31
LC 2	93	25	24	28	66	25	93	19	24	70	29	24
LC 3	47	46	38	85	108	21	29	48	14	18	17	36
LC 4	41	78	110	42	31	24	14	51	20	41	14	18
LC 5	19	32	71	34	23	97	24	100	32	27	24	62
LC 6	49	15	17	23	41	24	29	47	47	33	86	99

(b) Hexapod

Fig. 4. Limb assignment results.

4) Tegotae coefficients: We propose to compute the Tegotae coefficients $k_{i,j}$ from the learnt Jacobian matrix, and in particular from the $w_{LC_Z,m_{hip}}$ coefficients. Since these

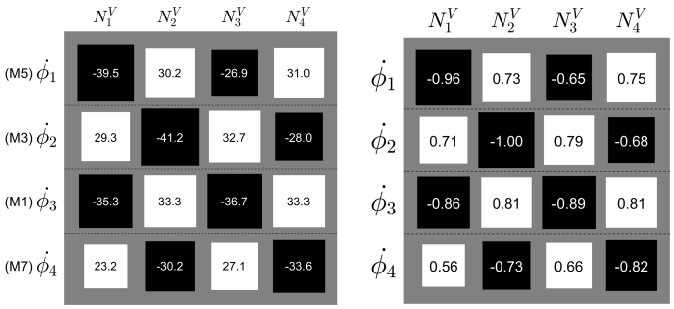

(a) Before renormalization (b) After renormalization

Fig. 5. Learnt Tegotae coefficients for quadruped.

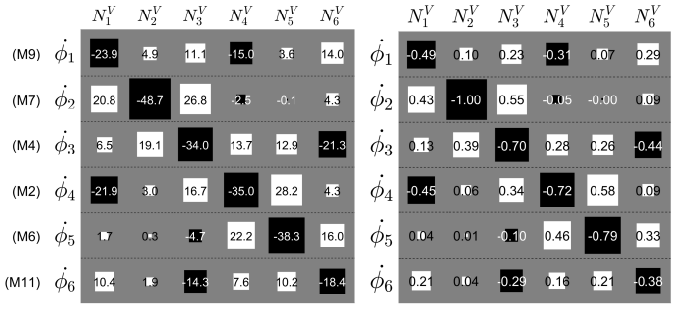

(a) Before renormalization (b) After renormalization

Fig. 6. Learnt Tegotae coefficients for hexapod.

coefficients represent the effect of the motors responsible for loading/unloading the limbs on the ground reaction forces under their own limb but also under the others, they can be used to synchronize the limbs using the ground reaction sensory feedback. We propose the following formula:

$$k_{i,j} = -sign(w_{LC_Z(i),m_{hip}(i)}) \cdot w_{LC_Z(j),m_{hip}(i)} \quad (8)$$

The $k_{i,j}$ are then normalized between +/- 1 so that only σ scales the effect of the sensory feedback compared to the descending drive in eq. (3). These coefficients form a square matrix $\mathbf{K}$ with dimensions n x n, where n is the number of limbs in the morphology. With this formula, the influence of the ground reaction force feedback under a limb j on the phase update of an other limb i depends on the effect of the unloading motor of the limb $m_{hip}(i)$ on that ground reaction force feedback. The first term is a sign correction coming from the mapping between the limb phase ϕ_i and the hip servomotor angle $\alpha_{hip(i)}$ (5). The Tegotae coefficients are presented in Fig. 5 for the quadruped and in Fig. 6 for the hexapod, each before and after renormalization.

For the quadruped, the Tegotae coefficients (see Fig. 5) exhibit a remarkable fully-connected checkerboard pattern which is consistent with the structure. Each limb feedback tend to put limb 1 and 3 in phase and limb 2 and 4 in opposite phase (either by accelerating or slowing them down together). For each line, the diagonal term is the highest (in absolute value) which means the feedback from the limb itself has the highest contribution, but each contribution has a relatively similar importance.

Compared to the Tegotae matrix of the quadruped structure, the Tegotae matrix learnt with the hexapod structure (Fig. 6) is much more sparse. This means that the couplings between motor movements and sensory reactions are more local and less globally connected than in the quadruped structure, which is quite intuitive. The information progression through the body is interesting: for each line, the highest contribution (in absolute value) is the diagonal term and the terms closest to 0 correspond to feedback from limbs which are distant from the considered limb. Yet there is a strong diagonal coupling between exterior limbs (limb 1 and 4, and limb 3 and 6).

IV. Experiments

The experiments aimed at assessing the locomotion behavior and performance of the quadruped and hexapod morphologies under the generalized Tegotae control, with the Tegotae coefficients extracted with the learning procedure described in section III-B. These coefficients are used in Eq. 3 which drives each limb. For all the locomotion results presented, the descending drive is set at $\omega = \pi$ rad/s ($= 0.5$ Hz), the oscillation amplitudes of both motors $a = b = 20°$, with an amplitude reduction to $a' = 4°$ for the hip motors when they are in stance (when ϕ is between π and 2π, see Fig. 1 for details). The limbs are all initialized with the same phase $\phi = 0$. The value of σ is chosen to scale an estimated sensory feedback term (the mean value of the diagonal Tegotae coefficients multiplied by the whole robot load) to half the value of the descending drive ω, i.e. $\omega/2 = \sigma \cdot tr(\mathbf{K})/n \cdot N_{robot}$.

A. Gait convergence

We investigated the gait convergence properties under matrix $\mathbf{K}$. The gait convergence time was estimated using the phase differences between the limbs and gait type was assessed by recording the load cell Z values. Once converged, the obtained gaits were recorded with Motion Capture to measure their speed and straightness (with the radius of curvature of the trajectory). The terrain was always flat and smooth.

B. Gait robustness

1) Initial conditions and perturbation: It has been shown by Owaki et al. [5] that the convergence depends on the initial limb phases if only local feedback is used (1) with an hexapod (which is not the case with the quadruped). The additional terms of (2) are required to obtain robustness to initial conditions with the hexapod. For both structures, random initial conditions were hence tested to control that the obtained gaits did not depend on initialization. Random manual perturbations (blocking a limb, adding load) were also applied during or after convergence. For the hexapod, initialization from a tripod synchronization (R1,L2,R3 initially at $\phi = 0$ and L1,R2,L3 initially at $\phi = \pi$) was also tested.

2) Loss of sensory feedback: The generalized Tegotae formula we propose uses all the sensory feedback available in the structure to compute the local phase update: this confers an increased robustness to noise and even to the absence of signal. On the other hand, with simple Tegotae, each load cell is needed to maintain their own limb's synchronization. The load sensory feedback is redundant in the sense that the loads under each limb are not independent. Relationships depending on the structure and its physical state constrain and link their values. We checked to what extent our generalized Tegotae coefficients incorporated that structural knowledge by testing the gait convergence with loss of sensory feedback. In these experiments, the "damaged"/"lost" load cells return a 0 value.

3) Loss of limb: We further tested this robustness by amputating legs of the hexapod. The limb amputation performed consists in electrically unplugging the limb servos, folding the limbs below the spine and putting its load cell signal to zero. The limbs are "amputated" in the sense that even if they are not physically removed from the structure, they cannot move or even hold the structure anymore. In both cases, we start with a fully functional hexapod and let it converge to the (R1L3)(R2L2)(R3L1) gait. We performed two amputation scenarios. In the first one, limbs R1 and L2 are amputated. In the second one, limbs R2 and L3 are amputated.

V. Results and Discussion

A. Gait convergence

1) Quadruped: The Tegotae coefficients presented Fig. 5b produce a trot gait (R1L2)(L2R1). As Fig. 7 shows, the convergence takes about 10 s (that is to say 5 cycles, given the 0.5 Hz frequency). Using the simple Tegotae rule instead (which is equivalent to replacing the matrix Fig. 5b by the diagonal identity matrix), the convergence takes about 30 s.

This trot gait is smooth (there are no brutal changes in limb phase from one update to an other) and quite effective in properly lifting its limbs: as Fig 7a shows, the front limbs R1 and L1 are completely unloaded (the ground reaction force falls to 0), while the hind limbs R2 and L2 are almost completely unloaded (they are trailing a bit because the robot is moving forward). It is straight, with a speed of 4.6 cm/s (see subsection V-A3 for details).

Given the Tegotae coefficients checkerboard pattern (see Fig. 5b), this convergence to trot is understandable: each feedback has the same effect (either slowing down or accelerating) on limb 1 and 3 and an opposite one on limb 2 and 4.

2) Hexapod: The Tegotae coefficients shown Fig. 6b produce a "bipod" gait (R1L3)(L2R2)(R3L1). The bipod gait, presented Fig. 8, is a gait where the two diagonal exterior limbs are paired together, and the central ones too. If the diagonal pairing of the exterior limbs can be understood as a direct effect of the Tegotae coefficients of Fig. 5b, the pairing of the central ones is an indirect one: the matrix only drives each central limb to be in phase opposition with the two limbs which are on its sides. The convergence takes about 25 s. Convergence to the same gait is obtained with different initial limb phases and stable in time, which is not the case with

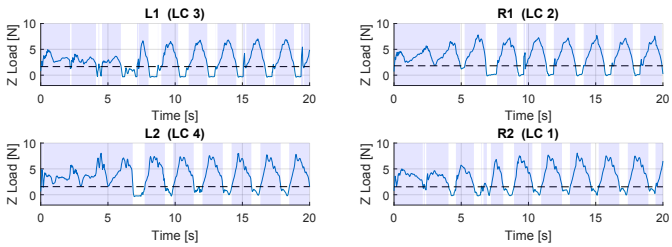

(a) Ground Reaction Forces measured by load cells

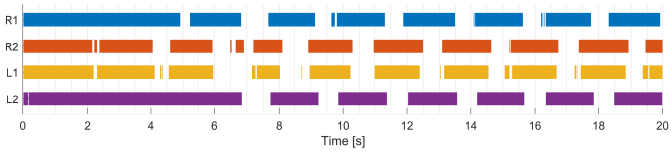

(b) Gait diagram

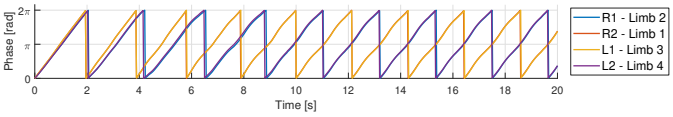

(c) Limb Phases computed by the board

Fig. 7. Generalized Tegotae convergence to trot (R1L2)(R2L1), obtained with the quadruped with the learnt Tegotae coefficients represented Fig. 5b.

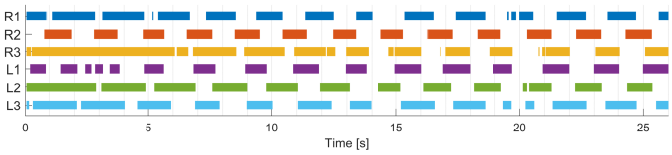

(a) Gait diagram

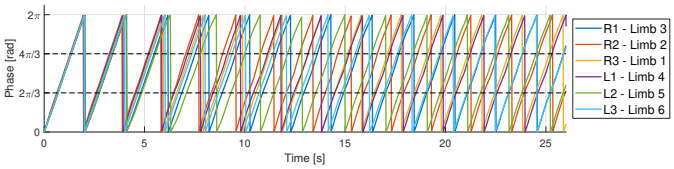

(b) Limb Phases computed by the board

Fig. 8. Convergence to "Bipod" (R1L3)(R2L2)(R3L1) gait, obtained for the hexapod with the learnt Tegotae coefficients represented Fig. 6b.

the local Tegotae rule (1), whose convergence depends on the hexapod initial state.

This gait is also smooth and all the limbs are completely lifted off. It is straight, with a speed of 5.6 cm/s (see subsection V-A3 for details). For the hexapod, it was harder to predict the gait considering the Tegotae coefficients (see Fig. 6b). The strong diagonal coupling between exterior limbs (between limb 1 "R3" and limb 4 "L1", and limb 3 "R1" and limb 6 "L3") pushes them to be in phase, which is observed in the bipod gait. This is probably where the pairing (R1L3) and (R3L1) in the bipod gait originates from. The lines from the central limbs (limb 2 "R2" and 5 "L2" on lines 2 and 5) push them to be in phase opposition with the limbs of the same side (respectively limb 1 and 3, and limb 4 and 6). This is probably why the central limbs (R2L2) move together.

This gait is not very animal-like. The central limbs (R2 and L2) move exactly in phase, in a sort of rowing movement: this breaks Wilson's second principle for insect locomotion that 'contralateral legs of the same segment alternate in phase' [16]. The bipod gait obtained with our hexapod however is very similar to the bipod gait proposed in [17] (comparing Fig. 8a to Fig. 4b in [17]). [17] shows that this gait is faster on flat terrains without adhesion (on a hexapod robot and in simulations of a Drosophila melanogaster) than the tripod gait observed in nature, which is faster when climb is required.

3) Speed and straightness: The speed and straightness were measured in order to assess that a basic controllability of the robot could be achieved with the emergent gaits. No optimality in terms of speed or straightness is claimed. The hardcoded gaits provide a baseline for the order of magnitude of speed and straightness that can be reasonably considered fast and straight enough. As Table I shows, the emergent gaits speed and straightness are of the same order of magnitude than their hardcoded counterparts. They are slightly slower because the sensory feedback contribution is still negative on a cycle average, even once converged.

TABLE I
SPEED AND STRAIGHTNESS: HARDCODED (HC) VS TEGOTAE (3).

	Quadruped Trot		Hexapod Bipod	
	HC	Fig. 5b	HC	Fig. 6b
Speed (cm/s)	4.9	4.6	6.2	5.6
Radius of Curvature (m)	5.8	7.6	37	8.5

B. Gait robustness

1) Initial conditions and perturbation: With both structures, the random initial conditions tested all converged to the same gaits (trot for quadruped and bipod for the hexapod). Likewise, the manual perturbations we applied did not result in convergence to different gaits. For the hexapod, the tripod initial conditions led to a significantly longer convergence time (approximately 50 s compared to 20 to 30 s for the others), but the robot still converged to the same bipod gait.

2) Robustness to less signal: With the quadruped structure, just one functioning load cell signal is enough to converge to a trot in approximately 30 s and maintain it. The coefficients which are used are the ones which were learnt with that same load cell: the other load cells could even have broken during the learning. With the hexapod structure, the matrix of Tegotae coefficients is not fully connected so it seems harder to maintain the synchronization of the whole structure with only one load cell. Yet, straight walking can be obtained with just one load cell signal: the results are summarized Table II.

3) Amputations: In both cases, there was a quick gait adaptation to trot with the remaining limbs: (R2L3)(R1L3) in the first case (see Fig. 9 (e2)) and (R1L2)(R3L1) in the second case. The two limbs which were synchronized with the amputated legs in the previously established bipod gait synchronize together (whereas they used to have a $2\pi/3$ phase shift), using the same Tegotae coefficients (learnt with the original fully functional structure) which had produced the bipod gait when all the limbs were functional. This amputation scenario shows that the emergent limb synchronization obtained with the learnt Tegotae coefficient can adapt to morphological changes and damages, by pairing limbs differently.

TABLE II
GENERALIZED TEGOTAE CONVERGENCE WITH ONLY ONE LOAD CELL SIGNAL KEPT FOR SENSORY FEEDBACK IN HEXAPOD STRUCTURE.

Loadcell kept	Generalized Tegotae Convergence
LC 1 (R3)	No straight gait
LC 2 (R2)	No straight gait
LC 3 (R1)	(R1L3)(R2R3L1), L2 not sync
LC 4 (L1)	(R3L1)(R1L2L3), R2 not sync
LC 5 (L2)	(R2L2)(R1L1L3), R3 not sync
LC 6 (L3)	(R1L3)(R2L1)(R3L2)

C. Limitations

For both robots, the twitching was performed with anti-slip rugs placed below the feet to improve the signals quality for better learning results. Without these rugs, the load cell signals would have required heavier signal processing for the weights to converge or more samples.

No optimality is claimed for any of the obtained gaits.

Neither of the morphologies exhibited gait transitions, either by changing the descending drive ω in (3) (limited to 1 Hz or $\omega = 2\pi rad/s$ due to the bandwidth of the servo motors) or by the sensory feedback gain σ.

VI. CONCLUSION AND FUTURE WORK

The learning method we developed combines the concept of spontaneous motor activity, Hebbian learning and Tegoate. It requires only a few minutes to collect samples and learn on board a Jacobian matrix between the motor twitching movements and the sensory responses. In the generalized version of Tegotae that we propose, the sensory feedback term is a limb-dependent linear combination of all the ground reaction forces from all the limbs. The coefficients of that combination can be computed from this learnt Jacobian matrix. Compared to simple Tegotae, it exhibits faster convergence to straight walking gaits, increased robustness to initialization and to a decrease of available sensory feedback. Gait adaptation to two-leg amputation was also demonstrated with generalized Tegotae and the coefficients learnt with our learning method. Our method was successfully applied to a quadruped and a hexapod. It still needs further testing on more exotic morphologies and leg designs. Likewise, further research is needed in the cases of multiple load cells per limb or actuated spine.

The implicit assumption of our method of exactly one load cell per limb simplified the Tegotae coefficient computing. However, the generalized Tegotae formula (3) theoretically does not require to have exactly one load cell per limb: each limb phase update is computed with coefficients learnt on its effect on the load cells, which could be extended to any number and location of load cells. This could include e.g. an actuated spine, an interesting path for future research. Likewise, the limb design with two servo motors in series

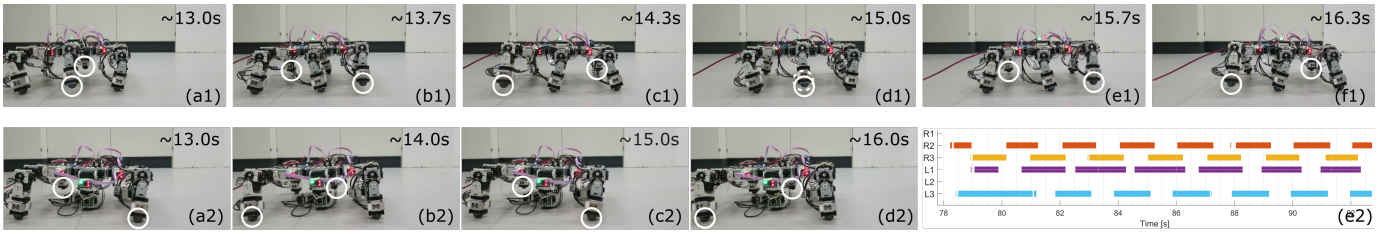

Fig. 9. Snapshots of the hexapod locomotion. (a1)-(e1) emergent bipod gait with two gait cycles, taking roughly 2 s each (0.5 Hz); (a2)-(d2) adapted trot gait after two leg amputations with two gait cylces, each taking 2 s. Legs in their swing phase are marked with white circles. The images are flipped with respect to the video to aid the understanding. (e2) Gait diagram of amputation convergence. Before $t = 78$ s, the fully functional hexapod had converged to a bipod gait. It was lifted off the ground to perform the limb amputations and set on the ground at $t = 78$ s, upon where the gait converges to a trot.

served as a simplification. The method is not limited to such designs, and applying it to higher actuated limbs (3 degrees of freedom and more) is also part of future research. Lastly, we do not make use of all the data collected in the Jacobian matrices. Yaw data from the gyroscope could be used to induce turning in the morphologies. We plan to extend the work with more such modalities and more morphologies.

Acknowledgments

This project is funded by the Swiss National Science Foundation (Project 200021_153299) and the Fundação para a Ciência e Tecnologia (FCT) agency of Ministry for Education and Science of Portugal (PD/BD/105781/2014).

References

[1] Sarah L Jarvis, Deanna R Worley, Sara M Hogy, Ashley E Hill, Kevin K Haussler, and Raoul F Reiser. “Kinematic and kinetic analysis of dogs during trotting after amputation of a thoracic limb”. In: *American journal of veterinary research* 74.9 (2013), pp. 1155–1163.

[2] Antoine Cully, Jeff Clune, Danesh Tarapore, and Jean-Baptiste Mouret. “Robots that can adapt like animals”. In: *Nature* 521 (May 2015).

[3] Josh Bongard, Victor Zykov, and Hod Lipson. “Resilient Machines Through Continuous Self-Modeling”. In: *Science* 314.5802 (2006), pp. 1118–1121.

[4] A Lundberg and CG Phillips. “T. Graham Brown’s film on locomotion in the decerebrate cat.” In: *The Journal of physiology* 231.2 (1973), 90P.

[5] Dai Owaki, Masashi Goda, Sakiko Miyazawa, and Akio Ishiguro. “A Minimal Model Describing Hexapedal Interlimb Coordination: The Tegotae-Based Approach”. In: *Frontiers in Neurorobotics* 11 (2017), p. 29.

[6] Takeshi Kano, Eiki Sato, Tatsuya Ono, Hitoshi Aonuma, Yoshiya Matsuzaka, and Akio Ishiguro. “A brittle star-like robot capable of immediately adapting to unexpected physical damage”. In: *Royal Society Open Science* 4.12 (2017), p. 171200.

[7] Dai Owaki, Takeshi Kano, Ko Nagasawa, Atsushi Tero, and Akio Ishiguro. “Simple robot suggests physical interlimb communication is essential for quadruped walking”. In: *Journal of The Royal Society Interface* 10.78 (2013), p. 20120669.

[8] Dai Owaki and Akio Ishiguro. “A Quadruped Robot Exhibiting Spontaneous Gait Transitions from Walking to Trotting to Galloping”. In: *Scientific Reports* 7.1 (2017), p. 277.

[9] Simon Hauser, Matthieu Dujany, Martijn van der Sar, Mehmet Mutlu, and Auke J. Ijspeert. “Learning to walk in arbitrary legged morphologies”. In: *9th International Symposium on Adaptive Motion of Animals and Machines (AMAM 2019)* (2019).

[10] Hugo Gravato Marques, Arjun Bharadwaj, and Fumiya Iida. “From Spontaneous Motor Activity to Coordinated Behaviour: A Developmental Model”. In: *PLOS Computational Biology* 10.7 (July 2014), pp. 1–20.

[11] Mark S. Blumberg, Cassandra M. Coleman, Ashlynn I. Gerth, and Bob McMurray. “Spatiotemporal Structure of REM Sleep Twitching Reveals Developmental Origins of Motor Synergies”. In: *Current Biology* 23.21 (2013), pp. 2100–2109.

[12] Per Petersson, Alexandra Waldenström, Christer Fåhraeus, and Jens Schouenborg. “Spontaneous muscle twitches during sleep guide spinal self-organization”. In: *Nature* 424.6944 (2003), pp. 72–75.

[13] Hugo Gravato Marques, Farhan Imtiaz, Fumiya Iida, and Rolf Pfeifer. “Self-organization of reflexive behavior from spontaneous motor activity”. In: *Biological Cybernetics* 107.1 (Feb. 2013), pp. 25–37.

[14] B Kosco. “Differential Hebbian Learning”. In: *AIP Conference Proceedings 151 on Neural Networks for Computing*. Snowbird, Utah, USA: American Institute of Physics Inc., 1987, pp. 277–282.

[15] Erkki Oja. “Simplified neuron model as a principal component analyzer”. In: *Journal of Mathematical Biology* 15.3 (Nov. 1982), pp. 267–273.

[16] Donald M Wilson. “Insect walking”. In: *Annual review of entomology* 11.1 (1966), pp. 103–122.

[17] Pavan Ramdya, Robin Thandiackal, Raphael Cherney, Thibault Asselborn, Richard Benton, Auke Jan Ijspeert, and Dario Floreano. “Climbing favours the tripod gait over alternative faster insect gaits”. In: *Nature Communications* 8.1 (2017), p. 14494.